

Implications of the ABC Resonance Structure on Elastic Neutron-Proton Scattering

Annette Pricking^{a,b}, M. Bashkanov^{a,b}, H. Clement^{a,b,*}

^aPhysikalisches Institut der Universität Tübingen, Germany

^bKepler Center for Astro and Particle Physics, University of Tübingen, Auf der Morgenstelle 14, D-72076 Tübingen, Germany

Abstract

In recent WASA-at-COSY measurements of the basic double-pionic fusion reactions $pn \rightarrow d\pi^0\pi^0$ and $pn \rightarrow d\pi^+\pi^-$ a narrow resonance structure with $I(J^P) = 0(3^+)$ in the total cross section has been found. If this constitutes a s -channel resonance in the pn system, then it should cause distinctive consequences in pn scattering. The magnitude of the decay width into the pn channel is estimated and the expected resonance effects in integral and differential pn scattering observables are presented. The inclusion of the resonance improves the description of total cross section data. For the analyzing power a characteristic energy dependence is predicted, which should allow a crucial experimental check of the resonance hypothesis.

Keywords: ABC resonance, pn scattering

1. Introduction

The so-called ABC-effect, which constitutes a peculiar low-mass enhancement in the invariant mass of an isoscalar pion pair produced in a double-pionic fusion reaction, has been a puzzle all the time since its first discovery fifty years ago by Abashian, Booth and Crowe [1]. Recent WASA-at-COSY experiments [2, 3] on the basic double-pionic fusion to deuterium established a tight correlation between the appearance of the ABC effect and a narrow Lorentzian energy dependence with mass $m = 2.37$ GeV and width $\Gamma = 70$ MeV in the integral cross sections of the reactions $pn \rightarrow d\pi^0\pi^0$ and $pn \rightarrow d\pi^+\pi^-$, isoscalar part. The differential distributions are consistent with a $I(J^P) = 0(3^+)$ assignment to this resonance-like structure. In addition the experimental Dalitz plots point to a $\Delta\Delta$ excitation in the intermediate state. Hence we consider the following reaction scenario for the interpretation of the data:

$$pn \rightarrow R \rightarrow \Delta\Delta \rightarrow (NN\pi\pi)_{I=0}, \quad (1)$$

where R denotes a s -channel resonance in pn and $\Delta\Delta$ systems. By this scenario we explicitly neglect a possible direct decay $R \rightarrow NN\pi$. Note that an intermediate $N\Delta$ configuration is excluded by isospin.

*corresponding author: H. Clement

Email address: clement@pit.physik.uni-tuebingen.de (H. Clement)

In this paper we consider the possible decay channels of such a resonance in the scenario of eq. (1). In particular we estimate the partial decay width into the elastic pn channel and calculate the effect of such a resonance onto the pn scattering observables.

2. Decay channels and widths

The cross section of the isoscalar two-body resonance process $pn \rightarrow R \rightarrow \Delta\Delta$ is given by

$$\sigma_{pn \rightarrow \Delta\Delta} = \frac{4\pi}{k_i^2} \frac{2J+1}{(2s_p+1)(2s_n+1)} \frac{m_R^2 \Gamma_i \Gamma_f}{(s-m_R^2)^2 + m_R^2 \Gamma^2}, \quad (2)$$

where k_i denotes the initial center-of-mass momentum.

With $J = 3$ and $s_p = s_n = 1/2$ the peak cross section at $\sqrt{s} = m_R = 2.37$ GeV ($k_i = 0.72$ GeV/c) is then

$$\sigma_{pn \rightarrow \Delta\Delta}(peak) = \sigma_0 \frac{\Gamma_i \Gamma_f}{\Gamma^2} \quad (3)$$

with

$$\sigma_0 = 16.4 \text{ mb (unitarity limit)}. \quad (4)$$

Since we also have

$$\Gamma = \Gamma_i + \Gamma_f, \quad (5)$$

we get from (3) and (5):

$$\Gamma_i = \Gamma \left(\frac{1}{2} \pm \sqrt{\frac{1}{4} - \frac{\sigma_{pn \rightarrow \Delta\Delta}(\text{peak})}{\sigma_0}} \right). \quad (6)$$

To estimate $\sigma_{pn \rightarrow \Delta\Delta}(\text{peak})$ consider the total cross sections of all channels, where the isoscalar $\Delta\Delta$ system can decay into:

- (i) $d\pi^0\pi^0$ and $d\pi^+\pi^-$:

Due to isospin rules we expect

$$\sigma_{d\pi^+\pi^-}(I=0) = 2 \sigma_{d\pi^0\pi^0}, \quad (7)$$

however, due to the isospin violation in the pion mass, the available phase space is somewhat smaller for charged pion production than for the production of the lighter neutral pions. In Ref. [3] it has been shown that this results in a resonance cross section, which is lower by about 20 % in case of the $d\pi^+\pi^-$ channel. Hence we have

$$\sigma_a := \sigma_{d\pi^+\pi^-} + \sigma_{d\pi^0\pi^0} \approx 2.6 \sigma_{d\pi^0\pi^0}. \quad (8)$$

The peak cross section of the $pn \rightarrow d\pi^0\pi^0$ reaction at $\sqrt{s} = 2.37$ GeV has been measured to be 0.27 mb [3]. This includes the contributions of the t -channel $\Delta\Delta$ and Roper excitations. Accounting for this background effect the pure resonance cross section in this channel amounts to about 0.24 mb, *i.e.*:

$$\sigma_a \approx 0.6 \text{ mb}. \quad (9)$$

- (ii) $np\pi^0\pi^0$, $np\pi^+\pi^-$ and $pp\pi^0\pi^-$ - only $I=0$ part:

In a recent paper [4] Fäldt and Wilkin present an estimate of the resonance cross section in the $pn \rightarrow pn\pi^0\pi^0$ reaction. According to their calculation based on final state interaction theory the expected peak cross section in the deuteron breakup channel $pn\pi^0\pi^0$ is about 85% that of the non-breakup channel $d\pi^0\pi^0$, *i.e.* about 0.2 mb. Very recently also Albaladejo and Oset [5] estimated the expected resonance cross sections in $pn \rightarrow pn\pi^0\pi^0$ and $pn \rightarrow pn\pi^+\pi^-$ using a more elaborate theoretical procedure. Their result for the $pn \rightarrow pn\pi^0\pi^0$ channel is compatible with that from Ref. [4].

Next we consider the $pp\pi^0\pi^-$ channel. Though both the pp pair and the $\pi^0\pi^-$ pair are isovector pairs, they may couple to $I=0$ in total. Hence the isoscalar resonance may also decay into the

isoscalar part of the $pp\pi^0\pi^-$ channel. In fact, the decay of the resonance into the $pp\pi^0\pi^-$ channel proceeds via the same intermediate $\Delta^+\Delta^0$ system as the $d\pi^0\pi^0$ channel does. From isospin coupling we expect that the resonance decay into the $pp\pi^0\pi^-$ system should be half that into the $np\pi^0\pi^0$ system. And since from the estimates in Ref. [4] we expect the resonance effect in the $np\pi^0\pi^0$ system to be about 0.20 mb, we estimate the peak resonance contribution in the $pp\pi^0\pi^-$ system to be in the order of 0.1 mb. In fact, a recent measurement [6] of this channel by WASA-at-COSY is in agreement with such a resonance contribution in the total cross section at $\sqrt{s} = 2.37$ GeV.

The resonance effect in the isoscalar part of the $np\pi^+\pi^-$ channel is composed of the configurations, where either both np and $\pi^+\pi^-$ pairs couple each to $I=0$ or both pairs each to $I=1$. The latter case provides the same situation as the $pp\pi^0\pi^-$ channel. Hence we have

$$\sigma_{np\pi^+\pi^-}(I=0) \approx 2\sigma_{np\pi^0\pi^0} + \sigma_{pp\pi^0\pi^-} \quad (10)$$

$$\begin{aligned} \sigma_b &:= \sigma_{np\pi^+\pi^-} + \sigma_{np\pi^0\pi^0} + \sigma_{pp\pi^0\pi^-} \\ &\approx 0.5 \text{ mb} + 0.2 \text{ mb} + 0.1 \text{ mb} \\ &\approx 0.8 \text{ mb}. \end{aligned} \quad (11)$$

We note that our estimate for the resonant $pn \rightarrow pn\pi^+\pi^-$ cross section is in agreement with that of Ref. [5].

- (iii) $pp\pi^-$ and $pn\pi^0$ ($I=0$ part):

The isoscalar part of single-pion production is not well known. Recent work [7, 8] suggests a maximum isoscalar cross section at $\sqrt{s} = 2.30$ GeV with an indication of some steep decline thereafter. At our resonance energy there are no data at all. Independent of this it is very hard to construct a process, where the intermediate $\Delta\Delta$ system decays by emission of a single pion only. In such a case one of the Δ excitations must be de-excited by pion exchange with the other Δ . However, the formation of an intermediate $N\Delta$ state is isospin forbidden – as already mentioned in the introduction. Also, the condition $J^P = 3^+$ is very hard to fulfill in such a scenario. Hence we conclude that any decay of the resonance R into these single-pion channels must be small compared to the favored decays into the two-pion channels.

Table 1: Branching ratios of the d^* resonance into its decay channels based on eqs. (3) and (12) and the peak cross sections given under (i) and (ii).

decay channel	branching ratio	remarks
np	10 %	predicted
$d\pi^0\pi^0$	15 %	measured
$d\pi^+\pi^-$	25 %	measured
$pp\pi^0\pi^-$	7 %	measured
$np\pi^+\pi^-$	31 %	predicted
$np\pi^0\pi^0$	12 %	predicted

Altogether we get as an estimate

$$\sigma_{pn \rightarrow \Delta\Delta}(peak) = \sigma_a + \sigma_b \approx 1.4(1) \text{ mb}. \quad (12)$$

Putting this into eq. (6) and selecting the minus sign before the root we obtain

$$\Gamma_i = 7(1) \text{ MeV} \quad \text{for } \Gamma = 70 \text{ MeV}, \quad (13)$$

which in turn corresponds to a resonance cross section in the elastic pn channel of only

$$\sigma_{pn \rightarrow pn} \approx 0.16 \text{ mb}, \quad (14)$$

if the resonance would contribute only incoherently.

From the peak cross sections given under (i) and (ii) as well as from eqs. (3) - (13) we may readily calculate the branching ratios $BR := \Gamma_j/\Gamma$ for the decay of the resonance into the channels j . The results are listed in Table 1.

The value obtained for Γ_i appears to be quite reasonable. It is somewhat smaller than the quark-model predictions of Ping et al. [9] (see their Table V) where they quote $\Gamma_i = 9 - 17 \text{ MeV}$. In this table they also quote a value of $\Gamma_i \leq 18 \text{ MeV}$ to be consistent with the SAID phase shift analysis SP07 [10]. An upper limit for Γ_i may be directly derived also from Table 2, where SAID cross sections are quoted for selected partial waves. Since $J^P = 3^+$, the initial partial waves for the formation of the resonance R are the 3D_3 and/or 3G_3 pn partial waves. The 3D_3 total elastic cross section at $T_p = 1.2 \text{ GeV}$ is 1.46 mb. Taking this as an upper limit for the elastic resonance cross section we obtain as an upper limit for the elastic decay width $\Gamma_i \leq 20 \text{ MeV}$. In case of a resonance excitation purely by the 3G_3 partial wave the total elastic cross section given by SAID for this partial wave is already exhausted by $\Gamma_i = 9 \text{ MeV}$. We note, however that we discuss here two extreme situations. Actually, 3D_3 and 3G_3 are J-coupled partial waves allowing for a mixing of both components. *I.e.*, the true solution may be in-between the two extreme cases, which we discuss in this paper for simplicity.

Table 2: Total, elastic and reaction cross sections for selected isoscalar pn partial waves at $T_p = 1.2 \text{ GeV}$ according to SAID [10].

partial wave	$\sigma_{tot}[\text{mb}]$	$\sigma_{tot}^{el}[\text{mb}]$	$\sigma_{tot}^{reac}[\text{mb}]$
3S_1	7.05	6.23	0.82
3D_1	4.51	3.17	1.34
3D_3	5.95	1.46	4.49
3G_3	1.30	0.25	1.05

We note in passing that the other solution of eq. (6) – the one with the +sign – leads to $\Gamma_i = 62 \text{ MeV}$ implying that the resonance would be predominantly elastic. *i.e.* mainly decaying into the elastic channel and only weakly decaying into the pion-production channels. This solution is at obvious variance with SAID.

Before we continue to discuss the consequences of the resonance hypothesis for the pn scattering observables, we shortly want to discuss the situation for the case that the spin-parity of the resonance would have been $J^P = 1^+$. As discussed in Ref. [2] a $\Delta\Delta$ system in relative s -wave in the intermediate state could in principle have $J^P = 1^+$ or 3^+ . In the $J^P = 1^+$ case we would get the unitarity limit $\sigma_0 = 7.0 \text{ mb}$ and using the estimate of Fäldt and Wilkin [4] $\sigma_{\Delta\Delta}(peak)/\sigma_0 = 0.31$. According to eq. (6) this leads, however, to an imaginary part for the partial width Γ_i in the pn channel. To avoid this imaginary part necessitates $\sigma_{\Delta\Delta}(peak) \leq 1.75 \text{ mb}$. This in turn means $\sigma_b \leq 0.85 \text{ mb}$, which is at variance with the estimates of Fäldt and Wilkin [4]. Taking this limiting case would result in $\Gamma_i = \Gamma/2 = 35 \text{ MeV}$ and $\sigma_{pn} = 1.75 \text{ mb}$. As already demonstrated by Fäldt and Wilkin [4] the estimated cross section for $J = 1$ exceeds the sum of the SAID inelastic cross sections in the 3S_1 and 3D_1 partial waves.

In general the decay widths of a resonance are momentum dependent. This is important, if we consider the resonance not only at its resonance mass – as done above – but also over a wider range of energies, as we will do now in the following. The momentum dependence is particularly significant for the numerator of the resonance amplitude, where the elastic decay width enters linearly and is highly momentum dependent due to the D - and G -wave character, respectively of the relevant partial waves. Following Ref. [11] we parameterize the elastic width due to the resonance excitation in the 3L_3 partial wave as follows:

$$\Gamma_i(q) = \Gamma_i \left(\frac{q}{q_R} \right)^{2L+1} \left(\frac{q_R^2 + \delta^2}{q^2 + \delta^2} \right)^{L+1}, \quad (15)$$

where q and q_R are the nucleon three-momenta in the rest-frame of the resonance at energies \sqrt{s} and m_R , re-

spectively. For the cutoff parameter we use $\delta = 0.5$ GeV/c².

In the exit channel the resonance decays into the $\Delta\Delta$ system with a relative s-wave between the two Δ s — as observed in the Δ angular distribution (Fig. 5 in Ref. [2]). Therefore we have

$$\Gamma_{\Delta\Delta} = g_{\Delta\Delta}^2 q_{\Delta\Delta} F(q_{\Delta\Delta})^2 \quad (16)$$

where a monopole form-factor

$$F(q_{\Delta\Delta}) = \frac{\Lambda^2}{\Lambda^2 + q_{\Delta\Delta}^2/4} \quad (17)$$

is introduced, in order to account for the ABC effect (see Refs. [2, 12]). The cutoff parameter Λ is adjusted for best reproduction of the ABC effect (low-mass enhancement) in the $M_{\pi\pi}$ spectrum. Since $q_{\Delta\Delta} = q_{\pi\pi}$, when neglecting the Fermi motion of the nucleons, this form-factor is reflected directly in the $M_{\pi\pi}$ spectrum and causes there the ABC effect by suppression of the high-mass region. Fitting the cutoff parameter Λ of this monopole form-factor to the data in the $M_{\pi\pi}$ spectrum results [2] in

$$\Lambda \approx 0.16 \text{ GeV}/c \quad (18)$$

corresponding to a length scale of $r = \frac{\hbar\sqrt{6}}{\Lambda} \approx 2$ fm.

The total width of the resonance is then given by

$$\Gamma_R(s) = \Gamma_i + \sum \Gamma_f = \Gamma_i(q) + \gamma_R \int dm_1^2 dm_2^2 q_{\Delta\Delta} F(q_{\Delta\Delta})^2 |D_{\Delta_1}(m_1^2) D_{\Delta_2}(m_2^2)|^2, \quad (19)$$

where the integral runs over all possible $q_{\Delta\Delta}$ and $N\pi$ -invariant mass-squared m_1^2 (m_2^2) forming the systems Δ_1 and Δ_2 , respectively [13].

The second term in eq. (18) denotes the decays of the resonance via the intermediate $\Delta\Delta$ system. The quantity γ_R contains the coupling constant $g_{\Delta\Delta}$ and other constants and is fitted to yield a total width of $\Gamma_R(s = m_R^2) = 70$ MeV.

3. Resonance amplitude in the pn channel

Knowing now the partial decay width of the resonance R into the elastic pn channel we can calculate the resonance effect in this channel by adding the resonance amplitude to the corresponding partial wave amplitude of the energy dependent SAID solution.

The scattering amplitude is given by the T-matrix elements for the (l, j) th partial wave, which are connected to those of the S-matrix by

$$T_{lj} = \frac{S_{lj} - 1}{2i}. \quad (20)$$

The S-matrix is parameterized usually in the Stapp notation [14]

$$S_{lj} = \eta_{lj} e^{2i\delta_{lj}} \quad (21)$$

where δ_{lj} denotes the real part of the phase shift in the (l, j) th partial wave and η_{lj} stands for its absorptive part, the inelasticity.

For the full partial wave amplitude in the resonating partial waves 3D_3 and 3G_3 , respectively, we take the product S-matrix approach as used for the SAID analysis of πN scattering [15]:

$$S_{lj} = S_{lj}^B \left(1 + 2i \frac{m_R \Gamma_i}{m_R^2 - s - im_R \Gamma_R} e^{2i\Phi_R} \right), \quad (22)$$

where S_{lj}^B denotes the non-resonating background contribution, for which we take the current SAID SP07 solution.

By doing so we assume that

- the energy-dependent SAID solution is not affected significantly by use of the data in the resonance region $T_n = (1.0 - 1.3)$ GeV. Since differential cross section data - as we will demonstrate below - show an insignificant sensitivity to the resonance, the only data of relevance in this region are the analyzing power data at $T_n = 1.1$ GeV. In a global SAID analysis based on a multitude of data such a single data set is not expected to play a significant role.
- the perturbation by the resonance amplitude is small, so that no severe problem with unitarity arises. Multiplication of the Breit-Wigner resonance term with the background S-matrix in the multiplicative S-matrix approach helps to diminish this problem. In case of $\Phi_R = 0$ unitarity is conserved by construction, otherwise one needs to check, whether for the resonating partial wave $\eta \leq 1$ is still valid.

In the resonance amplitude all values are fixed with the exception of the resonance phase Φ_R . There are a priori no predictions for this phase between resonance and background amplitudes. Hence it is treated as a free parameter. In the following we use the total pn cross section data to fix the resonance phase Φ_R .

4. Resonance effect in np scattering observables

The total (integral) elastic and reaction np cross sections are shown in Fig. 1. The solid curves give the current SAID solution and the dotted (dashed) lines the result, if we add the resonance amplitude in the 3D_3 (3G_3)

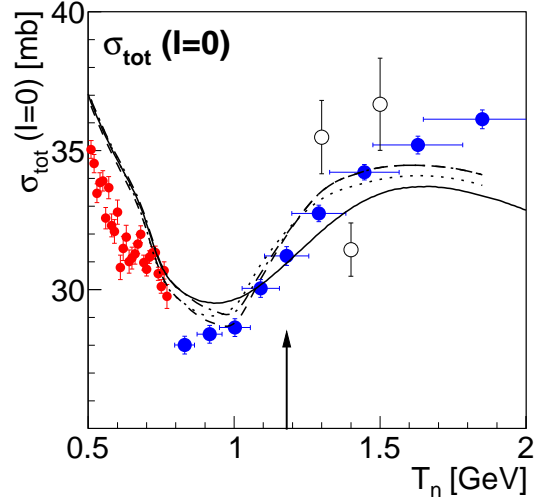
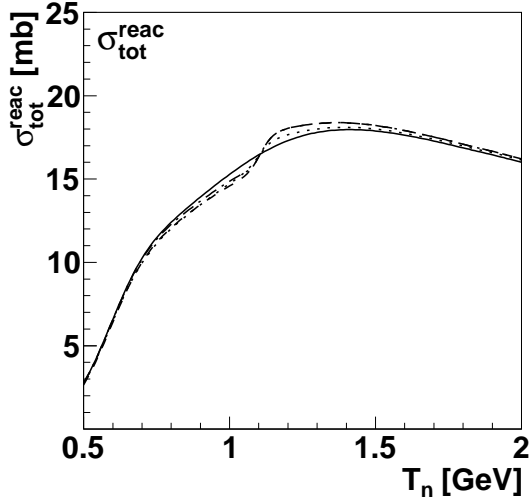
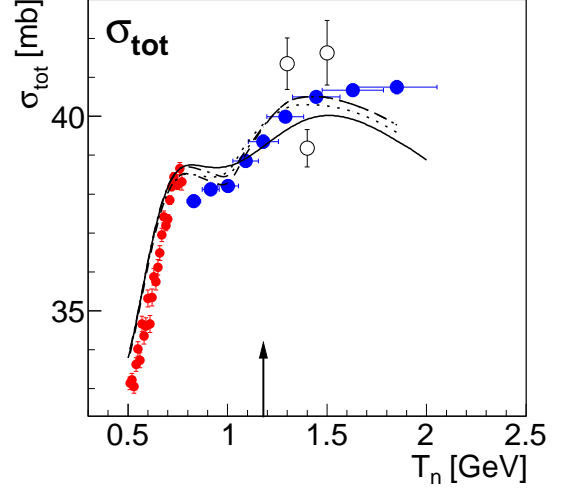
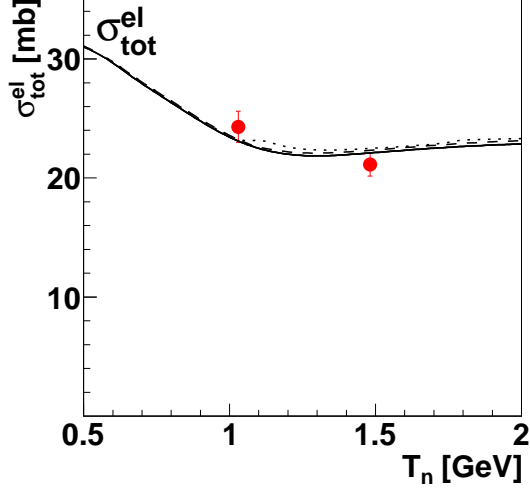


Figure 1: Total (integral) elastic (top) and inelastic (bottom) pn cross sections in dependence of the incident neutron energy T_n . The two data points are from Besliu et al. [16]. The solid lines denote the current SAID solution SP07 [10], the dotted (dashed) lines are the result, if we add the resonance amplitude in the 3D_3 (3G_3) partial wave. Note that dotted and dashed curves lie nearly on top of each other, since the total cross sections are not sensitive to the partial waves' orbital angular momenta. The dash-dotted curves are the result, if in the 3G_3 case the inelasticity η_{43} is constrained to unity, wherever it would exceed unity by adding the resonance amplitude. This concerns only the energy region $T_n < 1.1$ GeV.

Figure 2: Total pn cross section (top) and total isoscalar nucleon-nucleon cross section (bottom) in dependence of the incident neutron (nucleon) energy T_n . Data (solid symbols) below 800 MeV are from Lisowski et al. [17] and above 800 MeV from Devlin et al. [18]. The open symbols represent data from Sharov et al. [19]. The horizontal bars indicate the energy resolution of the incident neutrons. The plotted curves are averaged over these experimental energy resolutions. For the meaning of the curves see caption of Fig. 1. The vertical arrow indicates the position of the ABC resonance structure.

partial wave with phase $\Phi_R = -30^\circ$. As expected from the estimate in eq. (13), the resonance effect is very small in the integral cross sections. In addition there are no data to compare to with the exception of two data points with large uncertainties [16]. The experimental situation improves drastically, however, if we consider the sum of elastic and reaction cross section, *i.e.*, the full total np cross section, which can be accessed by 0° transmission measurements.

Fig. 2, top, shows the total np cross section for $T_n = (0.5 - 2)$ GeV. The data (solid symbols) plotted for $T_n < 0.8$ GeV are from Lisowski et al. [17] taken at LAMPF in a high-resolution dibaryon search. The data plotted for $T_n > 0.8$ GeV are from Devlin et al. [18] taken with a neutron energy resolution of (4–20)% (horizontal bars in Fig. 2). Also data from Sharov et al. [19] are shown (open symbols), which have larger uncertainties, but are taken with a much superior neutron energy resolution of (13 - 15) MeV. The data exhibit a pronounced jump in the cross section between $T_n = (1.0 - 1.3)$ GeV. This jump is remarkable, since the pp total cross section is completely flat in this energy region. Hence in the isoscalar total nucleon-nucleon cross section $\sigma_{I=0} = 2\sigma_{pn} - \sigma_{pp}$, where the SAID values are used for σ_{pp} , this jump appears still more pronounced (Fig. 2, bottom). The current SAID solution is shown by the solid lines again. Its description of the data is only fair. In particular the observed s -shaped increase in the total cross section above 1 GeV is only slightly indicated in the SAID solution.

If we include the resonance amplitude in the 3D_3 (3G_3) partial wave with a resonance phase $\Phi_R = 0$, then we obtain a Lorentzian shaped bump in the total cross section around $T_n \approx 1.1$ GeV, which roughly provides the right increase of the cross section in this energy region, but also a fall-off thereafter, which is not in accord with the data. To reproduce the s -shaped increase in the total cross section we rather need $\Phi_R \approx -(25 - 45)^\circ$, which provides a destructive interference with the 3D_3 (3G_3) background amplitude at energies below the resonance mass and a constructive interference above it. This calculation is shown in Fig. 2 by the dotted (dashed) lines. We see that the resulting s -shaped pattern improves significantly the agreement with the data. The calculations are averaged over the energy resolution of the neutron beams (indicated by the horizontal bars in Fig. 2) used in the experiments. This energy smearing is particularly large in the measurements of Devlin et al. [18].

Putting the resonance in either 3D_3 or 3G_3 partial waves makes no major difference here, since the total cross sections are not sensitive to the partial waves' or-

bital angular momenta. Slight differences arise from the fact that we have different momentum dependences for 3D_3 and 3G_3 partial waves — see eq. (15) — and in particular from the fact that the resonance amplitude is multiplied by the background amplitude — see eq. (22), where the real parts of 3D_3 and 3G_3 phase shifts differ by more than 10° .

The phase shifts for 3D_3 and 3G_3 partial waves in the energy region of interest are depicted in Fig. 3. For the 3D_3 -case the inclusion of the resonance with $\Phi_R \approx -(25 - 45)^\circ$ does not cause problems with unitarity, since the background inelasticity η_{23}^B is already much below unity in the energy region of the resonance.

For the 3G_3 -case the situation is much more delicate, since η_{43}^B is still close to unity in the resonance region — with the consequence that the total η_{43} gets slightly above unity for energies below 1.1 GeV. This points to the necessity that the background amplitudes would need to be readjusted, when taking into account the resonance explicitly. Since this would mean a major effort much beyond the scope of this work, where the main emphasis is to demonstrate the basic effect of the resonance on the observables, we demand for simplicity $\eta_{43} = 1$ in the region, where it would exceed unity. (Effectively, this means that we readjust the background inelasticity η_{43}^B accordingly.) This constrained calculation is shown in the figures by the dash-dotted lines. As expected, the calculation for the total cross sections falls now speedily back to the SAID solution in energy region below 1.1 GeV, where η_{43} is now constrained to unity. As we will show below in Fig. 5, this constraint has only tiny effects on the differential np -scattering observables at energies below 1.1 GeV.

After having succeeded in improving the description of the total cross section data substantially by inclusion of the resonance amplitude in 3D_3 or 3G_3 partial waves, we consider now the resonance effect in the differential observables. In contrast to the situation for the integral cross section, it will make here a substantial difference, whether the resonance is in the 3D_3 or the 3G_3 partial wave due to the different angular dependences of these partial waves — in particular in the analyzing power A_y , as we will demonstrate in the following.

Fig. 4 shows the angular distributions of differential cross section $d\sigma/d\cos(\Theta)$, vector analyzing analyzing power A_y and spin correlation coefficients A_{00ij} at $T_n = 1.13$ GeV corresponding to the resonance energy $\sqrt{s} = 2.37$ GeV, where we expect the effect of the resonance on the observables to be largest. At this energy there are only data for the differential cross section at small scattering angles. The solid lines denote the current SAID solution, the dotted (dashed) lines give the result with

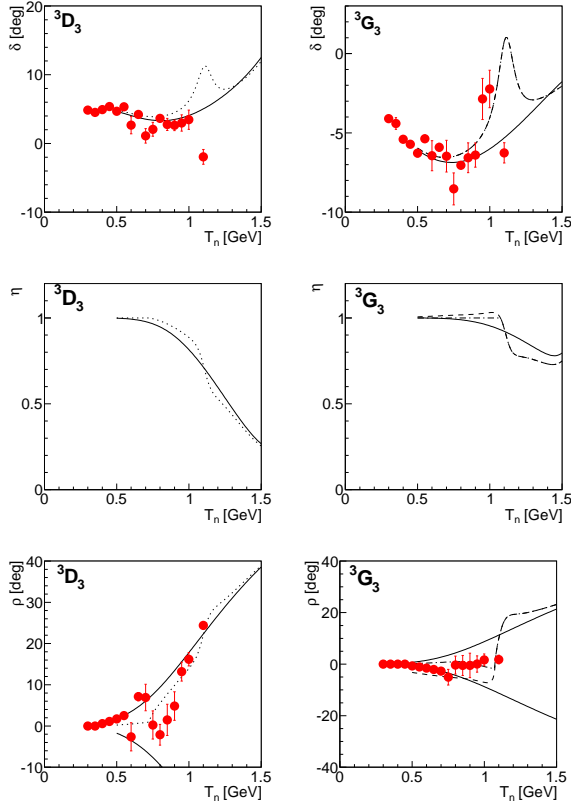


Figure 3: Energy dependence of the phase shifts for 3D_3 (left) and 3G_3 (right) partial waves. The real parts δ_{ij} are shown at the top, the imaginary parts below either as inelasticity η_{ij} (Stapp notation [14]) in the middle or as ρ_{ij} phase in the SAID convention [10, 22] at the bottom. The solid lines and symbols denote the SAID SP07 energy dependent and single energy solutions, respectively [10]. Since the sign of ρ does not enter [22], we plot the SAID solution for ρ for both signs. Dotted and dashed curves show the results of including the resonance amplitude in 3D_3 and 3G_3 partial waves, respectively. The dash-dotted curve results, if in the 3G_3 case the inelasticity η_{34} is constrained to unity, wherever it would exceed unity by adding the resonance amplitude. This concerns only the energy region $T_n < 1.1$ GeV.

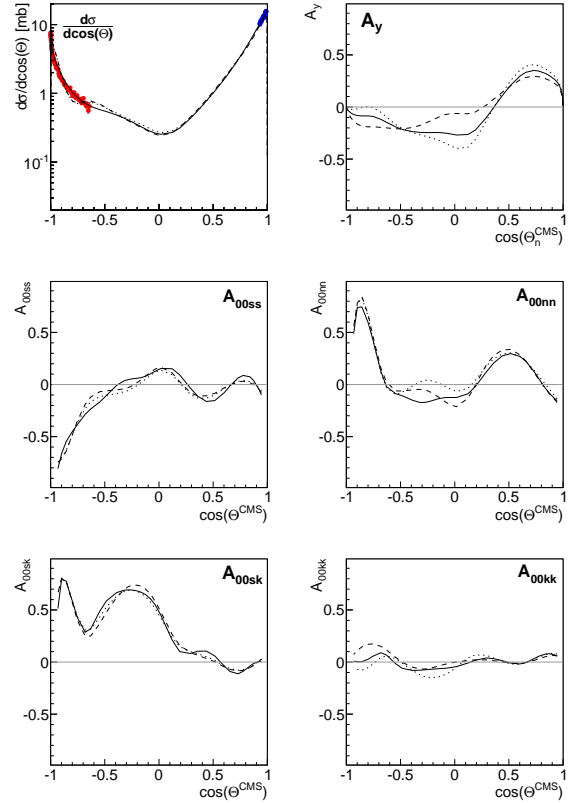


Figure 4: Differential distributions of cross section $d\sigma/d\cos(\Theta)$, vector analyzing power A_y and spin correlation coefficients A_{00ij} at $T_n = 1.13$ GeV corresponding to the resonance energy $\sqrt{s} = 2.37$ GeV. For the meaning of the curves see caption of Fig. 1. For the differential cross section data are plotted for the nearby energies $T_n = 1.118$ GeV [20] and $T_n = 1.135$ GeV [21].

the resonance amplitude added in the 3D_3 (3G_3) partial wave. As expected from the discussion of the integral elastic cross section the resonance effect is tiny in the differential cross section, however, sizably in the polarization observables. It is largest in the analyzing power A_y , which solely depends on interference terms. The resonance effects are particularly notable at intermediate angles, where the differential cross section gets smallest. We also see that 3D_3 and 3G_3 resonance contributions lead to opposite effects there. This provides the opportunity to disentangle these contributions by A_y measurements.

The decomposition of the np -scattering observables into partial wave amplitudes is given in Ref. [22]. Accordingly we have for the analyzing power:

$$d\sigma/d\cos(\Theta) * A_y \sim \text{Im}(H_3 + H_5)H_4^* \quad (23)$$

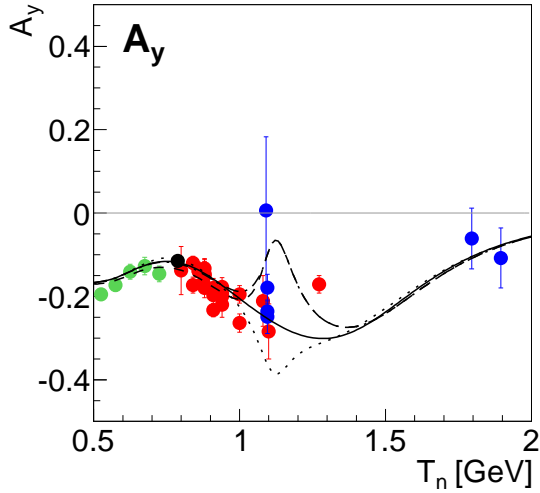


Figure 5: Energy dependence of the vector analyzing power at $\Theta_{cm} = 83^\circ$. The plotted data are from [23, 24, 25, 26, 27, 28, 29, 30, 31]. For the meaning of the curves see Fig. 1.

with H_i containing sums over partial wave amplitudes with total angular momenta $j_0 = j = L$, $j_- = L - 1$ and $j_+ = L + 1$. H_3 contains terms being proportional either to the Legendre polynomials P_j or to the associated ones P_j^1 . In H_5 there are terms only proportional to P_j and in H_4 only proportional to P_j^1 . In particular, the structure of H_4 for $j = 3$ is as follows:

$$H_4(j = 3) \sim [4(T_{L=4} - 3T_{L=2}) + \sqrt{12}T_{L=3}]P_3^1, \quad (24)$$

where the T-matrix elements contain the complex phase shifts. We see that a resonance effect in 3D_3 and 3G_3 enters with opposite sign and is proportional to P_3^1 in both cases. Hence the resonance effect vanishes at the zeros of P_3^1 , which is the case at $\cos(\Theta) = \pm 1/\sqrt{5} = \pm 0.447$ corresponding to $\Theta = 63.4^\circ$ and 116.6° . At these angles the predictions with and without resonance in 3D_3 or 3G_3 cross each other – see Fig. 4, top right. P_3^1 is maximal at $\cos(\Theta) = \pm\sqrt{11/15} = \pm 0.856$ and minimal at $\cos(\Theta) = 0$. Since at the latter the differential cross section is minimal and much lower than at $\cos(\Theta) = \pm 0.856$ – see Fig. 3, left –, the resonance effect in A_y gets maximal at $\cos(\Theta) = 0$, *i.e.* at $\Theta = 90^\circ$.

In Fig. 5 we plot the energy dependence of A_y near $\Theta = 90^\circ$, the angular region, where we find the largest resonance effects and where also a large amount of data are available, in particular from neutron-proton scattering experiments at Saclay [23, 24]. Since the angular dependence around $\Theta = 90^\circ$ is small, we plot in Fig. 5

the energy dependence at $\Theta = 83^\circ$, where the situation of available data [23, 24, 25, 26, 27, 28, 29, 30, 31] is more favorable than at $\Theta = 90^\circ$. The meaning of the drawn curves is the same as in Fig. 4. A significant resonance effect shows up within the energy region $T_n = (1.0 - 1.3)$ GeV. The effect is opposite in sign for the resonance residing in 3D_3 or 3G_3 partial waves. Note also that the calculations with (dashed) and without (dash-dotted) the constraint $\eta_{43} \leq 1$ exhibit only small differences for energies below 1.1 GeV – well within uncertainties of currently available data. This is not unexpected, since according to eqs. (20) - (24) the analyzing power is mainly sensitive to the real part of the phase shift.

5. Conclusions

Summarizing, we have shown that the $I(J^P) = 0(3^+)$ resonance structure found in the basic double-pionic fusion process $pn \rightarrow d\pi^0\pi^0$ is consistent with existing np scattering data. The effect of such a s -channel resonance is significant in specific np observables. In particular it improves considerably the description of the total cross section beyond 1 GeV. Among the differential observables the vector analyzing power exhibits the largest sensitivity to the resonance. However, for a crucial test of the resonance hypothesis and a meaningful separation of 3D_3 and 3G_3 resonance contributions high-precision data are needed for the energy region $T_n = (1.0 - 1.3)$ GeV. Such measurements have actually been carried out very recently with the WASA detector at COSY and the data analysis has started. The WASA detector installed at the COSY ring is particularly suited for analyzing power measurements in the intermediate angle region, which – as we have demonstrated here – is of main interest for the search of resonance effects in np scattering.

We finally note that on the issue of the $I(J^P) = 0(3^+)$ resonance structure meanwhile a first three-body Faddeev calculation with full relativistic kinematics and based on hadron dynamics has been carried out by Gal and Garzilaco [32]. They find, indeed, a resonance with just these quantum numbers at a mass of 2.36(2) GeV in agreement with the experimental observation.

6. Acknowledgments

We acknowledge valuable discussions on this matter with J. Haidenbauer, C. Hanhart, F. Hinterberger, A. Kacharava, I. Strakovsky, H. Ströher, G.J. Wagner, C. Wilkin, A. Wirzba and R. Workman. We are indebted

to C. Elster for using her partial wave code by one of us (A.P.). This work has been supported by the BMBF (06TU9193) and the Forschungszentrum Jülich (COSY-FFE).

References

- [1] A. Abashian, N. E. Booth, K. M. Crowe, *Phys. Rev. Lett.* **6**, 258 (1960); **7**, 35 (1961); *Phys. Rev. C* **132**, 2296ff (1963)
- [2] P. Adlarson et al., *Phys. Rev. Lett.* **106**, 242302 (2011)
- [3] P. Adlarson et al., *Phys. Lett. B* **721**, 229 (2013); arXiv: 1212.2881 [nucl-ex]
- [4] G. Fäldt and C. Wilkin, *Phys. Lett. B* **701**, 619 (2011); arXiv: 1105.4142 [nucl-th]
- [5] M. Albadejo and E. Oset, *Phys. Rev. C* **88**, 014006 (2013)
- [6] P. Adlarson et al., submitted for publication; arXiv: 1306.5130 [nucl-ex]
- [7] V. V. Sarantsev et al., *Eur. Phys. J. A* **21**, 303 (2004)
- [8] V. V. Sarantsev et al., *Eur. Phys. J. A* **43**, 11 (2010)
- [9] J. L. Ping et al., *Phys. Rev. C* **79**, 024001 (2009)
- [10] SAID data base <http://gwdac.phys.gwu.edu/>; R. A. Arndt et al., *Phys. Rev. C* **76**, 025209 (2007).
- [11] S. Teis et al., *Z. Phys. A* **356**, 421 (1997)
- [12] M. Bashkanov et al., *Phys. Rev. Lett.* **102**, 052301 (2009)
- [13] C. Hanhart, priv. comm.
- [14] H. P. Stapp, R. Ypsilantis, N. Metropolis, *Phys. Rev.* **105**, 302 (1957)
- [15] R. A. Arndt et al., *Phys. Rev. C* **69**, 035213 (2004)
- [16] Besliu et al., *Sov. J. Nucl. Phys.* **43**, 888 (1986)
- [17] P. W. Lisowski et al., *Phys. Rev. Lett.* **49**, 255 (1982)
- [18] T. J. Devlin et al., *Phys. Rev. D* **8**, 136 (1973)
- [19] V. I. Sharov et al., *Eur. Phys. J. C* **37**, 79 (2004)
- [20] G. Bizard et al., *Nucl. Phys. B* **85**, 14 (1975)
- [21] Y. Terrien et al., *Phys. Rev. Lett.* **59**, 1534 (1987)
- [22] R. A. Arndt et al., *Phys. Rev. D* **28** (1983) 97 and references therein
- [23] J. Ball et al., *Nucl. Phys. A* **559**, 489 (1993); *ibid.* 477 and 511
- [24] A. de Lesquen et al., *Eur. Phys. J. C* **11**, 69 (1999)
- [25] Newsom et al., *Phys. Rev. C* **39**, 965 (1989)
- [26] Arnold et al., *Eur. Phys. J. C* **17**, 67 (2000)
- [27] J. Ball et al., *Nucl. Phys. B* **286**, 635 (1987)
- [28] McNaughton et al., *Phys. Rev. C* **48**, 256 (1993); **C 53**, 1092 (1996)
- [29] M. Sakuda et al., *Phys. Rev. D* **25**, 2004 (1982)
- [30] Glass et al., *Phys. Rev. C* **47**, 1369 (1993)
- [31] Y. Makdisi et al., *Phys. Rev. Lett.* **45**, 1529 (1980)
- [32] A. Gal and H. Garcilazo, *Phys. Rev. Lett.* in press; arXiv:1308.2112 [nucl-th]